Langmuir

Article

pubs.acs.org/Langmuir

Dynamic Light Scattering Study and DLVO Analysis of Physicochemical Interactions in Colloidal Suspensions of Charged Disks

Debasish Saha,[†] Ranjini Bandyopadhyay,*[,†] and Yogesh M. Joshi*[,‡]

[†]Soft Condensed Matter Group, Raman Research Institute, C. V. Raman Avenue, Sadashivanagar, Bangalore 560 080, India

[‡]Department of Chemical Engineering, Indian Institute of Technology Kanpur, Kanpur 208 016, India

Supporting Information

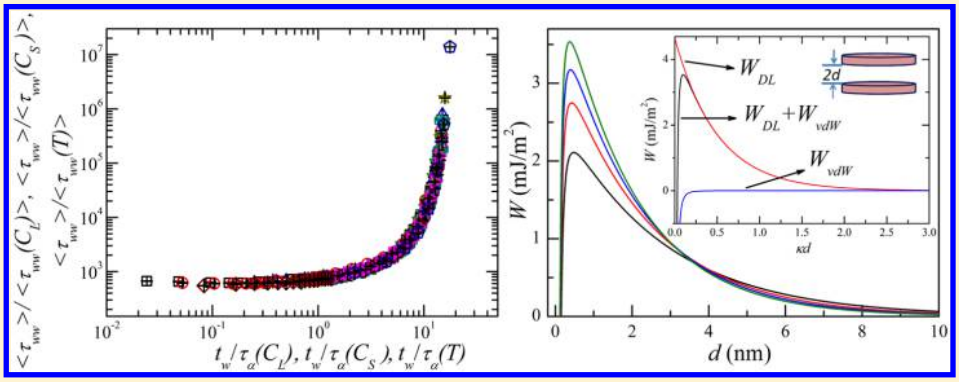

ABSTRACT: The interparticle interactions in colloidal suspensions of charged disks of Laponite clay in water were investigated using dynamic light scattering (DLS) and Derjaguin−Landau−Verwey−Overbeek (DLVO) theory. We studied the effects of clay concentration (C_L), the concentration of externally added salt (C_S), and temperature (T) on the microscopic dynamics of the clay suspensions. The fast (τ_1) and mean slow relaxation times ($\langle\tau_{ww}\rangle$) of Laponite suspensions were extracted from intensity autocorrelation functions measured at different waiting times (t_w) after sample preparation. Comprehensive Laponite concentration−salt concentration−temperature−time superpositions of both the microscopic diffusive time scales and the stretching exponent corresponding to the slow relaxation process highlight the self-similar nature of the energy landscapes of the Laponite suspensions. The evolution of the sodium ion concentration in the aging suspension with t_w, measured for several values of C_L, C_S, and T, was used in a DLVO analysis of the free energy of the suspension for two charged disks parallely approaching one another. This analysis confirms that, in addition to repulsive interparticle interactions, attractive interactions also play a pivotal role in the microscopic dynamics of spontaneously evolving Laponite suspensions.

INTRODUCTION

Interparticle interactions in colloidal dispersions determine their microstructures, which, in turn, influence their physical properties. In the limit of small concentrations, colloidal particles scarcely interact with each other, with the dispersions existing in the liquid state. Upon increasing the concentration, enhanced interparticle interactions can lead to self-assembled structures that strongly depend upon the charges and shapes of the particles.[1,2] The complexity of the structure is expected to increase if the particles possess dissimilar charges and anisotropic shapes.[3] Moreover, in some cases, the spontaneously formed structures may not be in thermodynamic equilibrium and can continue to evolve with time over the observation time scales.[4] In this article, we study the relaxation dynamics of aqueous colloidal dispersions of the smectite clay, Laponite. Laponite particles are characterized by their anisotropic shapes, dissimilar charges, and time-dependent structures in aqueous suspensions even at very small particle concentrations.[3]

Hydrous sodium lithium magnesium silicate ($Na_{+0.7}[(Si_8Mg_{5.5}Li_{0.3})O_{20}(OH)_4]_{-0.7}$), or Laponite, is a hectorite clay with a disk-like shape (diameter, 25 ± 2.5 nm; thickness, approximately 1 nm).[5] When dispersed in aqueous media, the sodium ions from the interlayer galleries dissociate, with the two faces of the Laponite particle acquiring negative charges.[6] The edge of the particle is composed of anhydrous oxides dominated by MgOH groups. Incorporation of Laponite powder in ultrapure water raises its pH due to the dissociation of OH^- ions from the edges and leads to the edges acquiring positive charges.[6,7] Owing to dissimilar charges on their edges and faces, the particles can interact via attractive as well as

Received: January 23, 2015
Revised: March 1, 2015
Published: March 2, 2015

DOI: 10.1021/acs.langmuir.5b00291
Langmuir 2015, 31, 3012−3020

repulsive interactions, thereby strongly influencing the sample's microstructure.[8−10] Addition of monovalent salts such as NaCl in aqueous suspensions of Laponite increases the concentrations of cations and anions that shield the charges on the particles and effectively reduces the interparticle repulsive interactions. Typically, for Laponite suspensions with concentrations C_L above 2 wt %, the viscosity, elastic modulus, and relaxation times increase gradually as a function of time since their preparation.[11−13] This suggests a continuous buildup of structure in a process that is referred to as physical aging.[14−16] The application of a deformation field can reverse the process of aging, with the viscosity, elastic modulus, and relaxation time decreasing due to the breakdown of the sample's microstructure.[15,17−19]

The phase behavior of aqueous suspensions of Laponite has been studied using static and dynamic light scattering,[13,20−27] small-angle X-ray scattering,[28] microscopy,[29] and rheology.[30−34] There is a general consensus that for C_L < 2 wt % (approximately) the microstructure is dominated by edge-to-face attractive interactions, leading to an attractive gel.[8,35] For higher concentrations, there is debate regarding whether the particles are in mutual contact due to attractive interactions or remain self-suspended in the repulsive environments of the surrounding particles, thereby forming a repulsive glass.[30,35] Small angle X-ray scattering (SAXS) of Laponite suspensions showed that the average interparticle distance increases from 15 nm for C_L < 2 wt % to 40 nm for high concentrations,[28] indicating the presence of an attractive gel-like morphology at low concentrations and a repulsive glass-like microstructure at high concentrations. Dissolution experiments[36] showed that Laponite suspensions that were older than 7 days do not dissolve in aqueous medium, thereby suggesting that the influence of attractive interactions on the microstructures of old samples cannot be ignored. By monitoring the evolution of the elastic moduli of shear-melted Laponite suspensions for samples of different concentrations (C_L), added salt concentrations (C_S), temperatures (T), and times (t_i) at which shear melting was carried out after sample preparation, it was demonstrated that older shear-melted suspension have larger elastic moduli than those of the young shear-melted ones.[30,31] This indicates that the permanent structures in aged Laponite suspensions cannot be destroyed even by applying very large shear deformations. Ionic conductivity measurements and DLVO calculations for various electrostatic screening conditions[30] showed that the influence of attractive interactions in older Laponite suspensions cannot be ignored and are in close agreement with the observations of the dissolution experiments.[36]

In this article, we employ dynamic light scattering (DLS) to study the relaxation dynamics of spontaneously evolving Laponite suspensions. These dynamics are studied by controlling all three physicochemical variables, C_L, C_S, and T. The spontaneously evolving Laponite suspensions used here are less than 3 days old (t_w < 3 days) and therefore are comparatively younger than the samples that were used for the rheological studies mentioned earlier.[30] We extract the evolution of the relaxation time scales of Laponite suspensions from our DLS data to understand the complex aging dynamics of the samples. To gain further insight into the dynamics and microstructures, we measure the ionic strengths of the samples and analyze the physicochemical interactions in Laponite suspensions using the DLVO theory.

SAMPLE PREPARATION AND EXPERIMENTAL METHODS

Laponite (Laponite RD) was procured from Southern Clay Products. Since Laponite is hygroscopic, the powder was dried for up to 16 h at 120 °C in an oven. Dried Laponite was added to Millipore water (resistivity 18.2 MΩ-cm) and stirred vigorously using a magnetic stirrer until the suspension appeared optically clear. A syringe pump (Fusion 400, Chemyx Inc.) and a 0.45 μm Millipore Millex-HV syringe-driven filter unit were used to filter the suspension at a constant flow rate of 3.0 mL/min. A sodium chloride (NaCl procured from Sigma-Aldrich) solution of a predetermined concentration was added to the filtered Laponite suspension using a pipet. The suspension was vigorously stirred during addition of the salt solution. The sample was then filled and sealed in a cuvette for the DLS experiments. The waiting time or the aging time, t_w, was calculated from the moment the sample was sealed. A Brookhaven Instruments Corporation (BIC) BI-200SM spectrometer was used to study the samples. A 532 nm solid-state laser ($NdYVO_4$, Coherent Inc., Spectra Physics) with an output intensity of 150 mW was used in the experiments to achieve a high scattered photon count. The scattering angle was fixed at 90° for all of the experiments reported here. The temperature of the suspension was maintained at the desired value by water circulation with a temperature controller (Polyscience Digital) attached to the DLS setup. The intensity autocorrelation function of the scattered light, $g^{(2)}(t)$, defined as $g^{(2)}(t) = \langle I(0)I(t)\rangle/\langle I(0)\rangle^2 = 1 + A|g^{(1)}(t)|^2$, was measured using a digital autocorrelator (Brookhaven BI-9000AT).[37] Here, $I(t)$ is the intensity of the scattered light at a delay time t, $g^{(1)}(t)$ is the normalized electric field autocorrelation function, and A is the coherence factor. We also estimate Na^+ concentration as a function of t_w using a Eutech CyberScan 2100 pH/ion meter equipped with a sodium ion selective electrode (ROSS Sure-Flow). The details of the measurements are provided in the Supporting Information. Zeta potential of the Laponite suspension, measured using a Malvern Zetasizer Nano Z zeta potential analyzer, is discussed in Supporting Information. The concentration measurements (in % w/v) refer to the weight of Laponite in grams that is mixed in 100 mL (100 g) of Millipore water.

RESULTS AND DISCUSSION

The evolution of the relaxation time of an aging Laponite suspension was estimated by analyzing the intensity autocorrelation function $g^{(2)}(t)$ for different waiting times, t_w, after the sample was sealed in the cuvette. The normalized intensity autocorrelation function, $C(t) = g^{(2)}(t) - 1$, as a function of delay time t for a 3.0% w/v Laponite suspension with 0.05 mM salt concentration at 15 °C is plotted in Figure 1 for different waiting times t_w. It is observed from Figure 1 that the decay in $C(t)$ slows with increasing t_w. Furthermore, $C(t)$ exhibits a two-

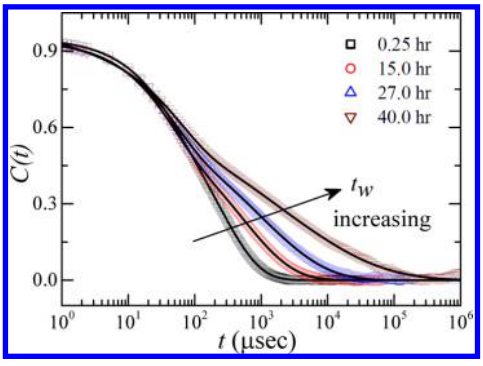

Figure 1. Normalized intensity autocorrelation functions $C(t)$ vs delay time t at 15 °C and a scattering angle θ = 90° for a 3.0% w/v Laponite suspension with 0.05 mM salt at several t_w. The solid lines are fits to eq 1.

DOI: 10.1021/acs.langmuir.5b00291
Langmuir 2015, 31, 3012−3020

step decay, which is typical of glass-forming materials as they approach the glass transition.[38]

For a molecular glass former where the glass transition is driven by a rapid decrease in temperature, the faster β-relaxation process shows an Arrhenius temperature dependence, whereas the slower structural α-relaxation process exhibits a Vogel−Fulcher−Tammann (VFT) temperature dependence.[39−41] In a recent publication, it was shown that the glass transition of spontaneously evolving Laponite suspensions is waiting time (t_w) driven and can be compared to the glass transition of supercooled liquids by a one-to-one mapping between the waiting time (t_w) of the former and the inverse of the temperature ($1/T$) of the latter.[20] Details are provided in the Supporting Information. The two-step relaxation in $C(t)$ shown in Figure 1 can be expressed as follows[20,42,43]

$$C(t) = [a \exp\{-t/\tau_1\} + (1 - a) \exp\{-(t/\tau_{ww})^{\beta}\}]^2 \quad (1)$$

Equation 1 fits all of the autocorrelation data acquired in DLS experiments for Laponite suspensions characterized by different C_L, C_S, and T. In all of the fits, a, τ_1, τ_{ww}, and β are the fitting parameters. It is seen from the fits that the relaxation time τ_1 associated with the exponential relaxation process is always faster than the slow relaxation time τ_{ww}. τ_1 is therefore associated with the fast relaxation process of the soft glassy Laponite suspension and is believed to arise from the motion of particles within cages formed by their neighbors.[44] The intercept a is a measure of the relative strength of this fast relaxation process. The slow nonexponential relaxation process, which yields the slow relaxation time τ_{ww}, is associated with the cooperative diffusion of a particle out of its cage.[11,20,42] The mean value of τ_{ww} is defined by $\langle\tau_{ww}\rangle = (\tau_{ww}/\beta)\Gamma(1/\beta)$,[45] where β is the stretching exponent ($\beta < 1$) and Γ is the Euler Gamma function.

In Figure 2a, $\langle\tau_{ww}\rangle$ is plotted as a function of t_w for Laponite suspensions of several different C_L with C_S = 0.05 mM at T = 25 °C. It is apparent from the figure that the time evolution of $\langle\tau_{ww}\rangle$ possesses self-similar curvatures at different Laponite concentrations. The superposition of the slow relaxation times, achieved by suitably normalizing both axes by shift factors for different C_L, and the horizontal and vertical shift factors are plotted in Figure S1. In Figure 2b, we plot $\langle\tau_{ww}\rangle$ vs t_w for Laponite suspensions having different C_S with C_L = 3.0% w/v at T = 25 °C. In Figure 2c, we plot the evolution of $\langle\tau_{ww}\rangle$ with t_w for Laponite suspensions of C_L = 3.0% and C_S = 0.05 mM at several T. Clearly, all of the plots in Figure 2b,c also show self-similar curvatures. The superpositions of the data for samples with different C_S and T and the corresponding shift factors used for the superpositions are plotted in Figure S1c−f.

Similar to the data for $\langle\tau_{ww}\rangle$, τ_1 and β are also observed to be very sensitive to C_L, C_S, and T (Figures 3 and 4). A comparison of the data in Figures 2 and 3 reveals that the increase in $\langle\tau_{ww}\rangle$ with t_w is much stronger than for τ_1 for all of the samples investigated here. This results in a separation of the α and β relaxation time scales as the sample ages, with the two-step relaxation process being very clearly visible for the older samples (Figure 1). It is seen from Figure 4 that β decreases linearly with t_w when C_L, C_S, and T are changed. As in the case of $\langle\tau_{ww}\rangle$, τ_1 and β also show self-similar time evolution when C_L, C_S, and T are varied. This is seen in Figures S2a−f and S3a−f. With increasing C_L, C_S, and T, the time evolution of $\langle\tau_{ww}\rangle$, τ_1, and β shift to smaller t_w, indicating an increase in the rate of structure buildup with increasing values of the physicochemical variables. Interestingly, for a given C_L, C_S, and T, the horizontal shift factors used to superpose the $\langle\tau_{ww}\rangle$ and β data (plotted in Figures S1 and S3) are approximately the same.

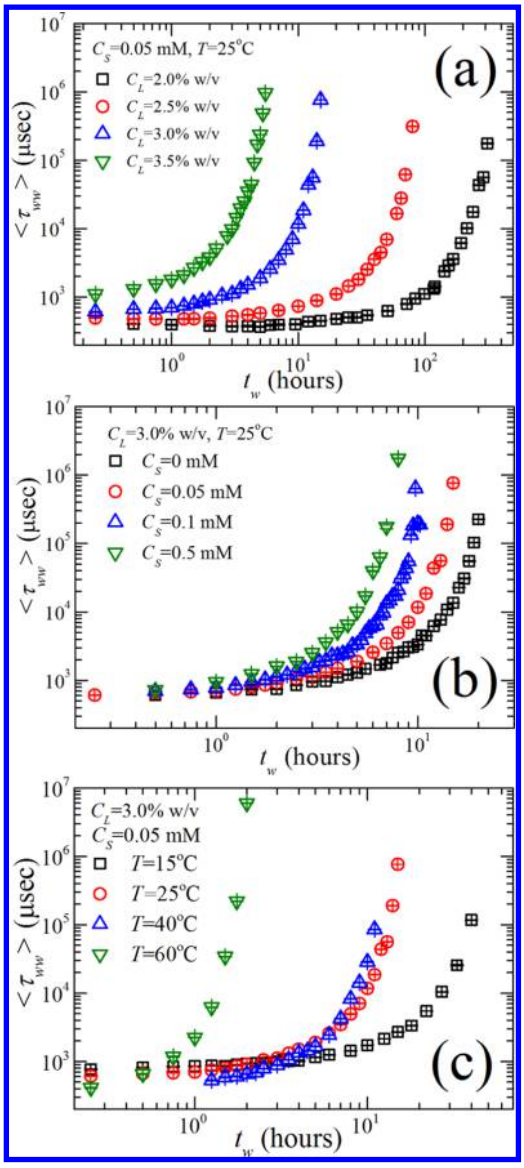

Figure 2. Mean slow relaxation times $\langle\tau_{ww}\rangle$, obtained by fitting the $C(t)$ data to eq 1, plotted vs t_w for different (a) C_L, (b) C_S, and (c) T values.

In Figure 5a, we plot the comprehensive Laponite concentration−salt concentration−temperature−time superpositions of the $\langle\tau_{ww}\rangle$ data (Figure 2). Similar comprehensive overlaps are also observed for τ_1 (Figure 3) and β (Figure 4) and are shown in Figure 5. The excellent superpositions suggest that the temporal evolution of the relaxation processes in Laponite suspensions is self-similar when C_L, C_S, and T are varied, indicating that the underlying energy landscapes remain self-similar when these variables are changed. These results are similar to the ones reported earlier for significantly old, rejuvenated Laponite suspensions.[30] The results reported here, therefore, demonstrate that the time evolution of the relaxation processes remains similar in young and old Laponite samples. This is attributed to the fact that, whatever the initial state of the sample, the process of structural buildup is dictated only by the interactions that the particles share among themselves.

DOI: 10.1021/acs.langmuir.5b00291
Langmuir 2015, 31, 3012−3020

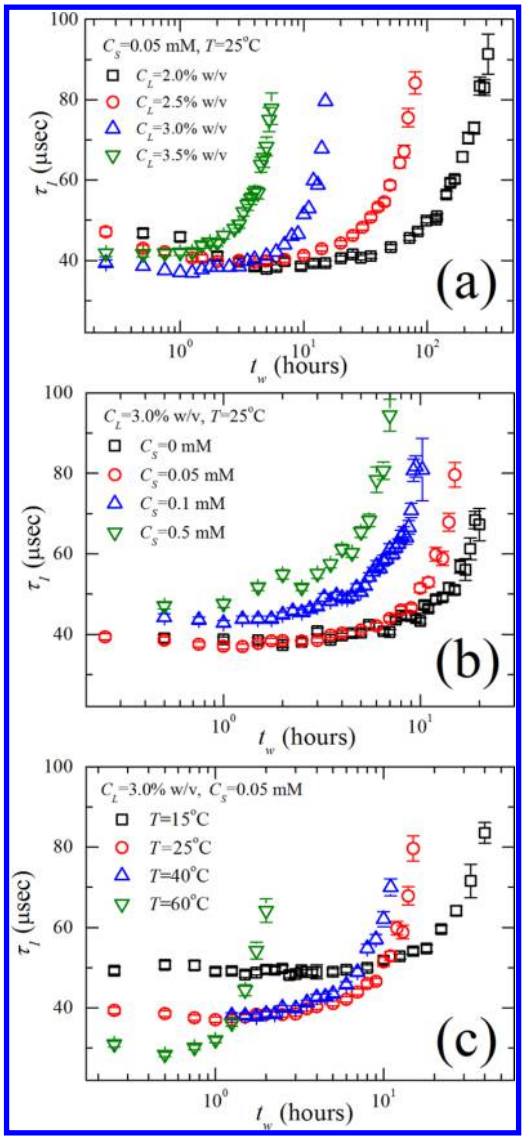

Figure 3. Fast relaxation times τ_1 plotted vs waiting times t_w for different (a) C_L, (b) C_S, and (c) T values.

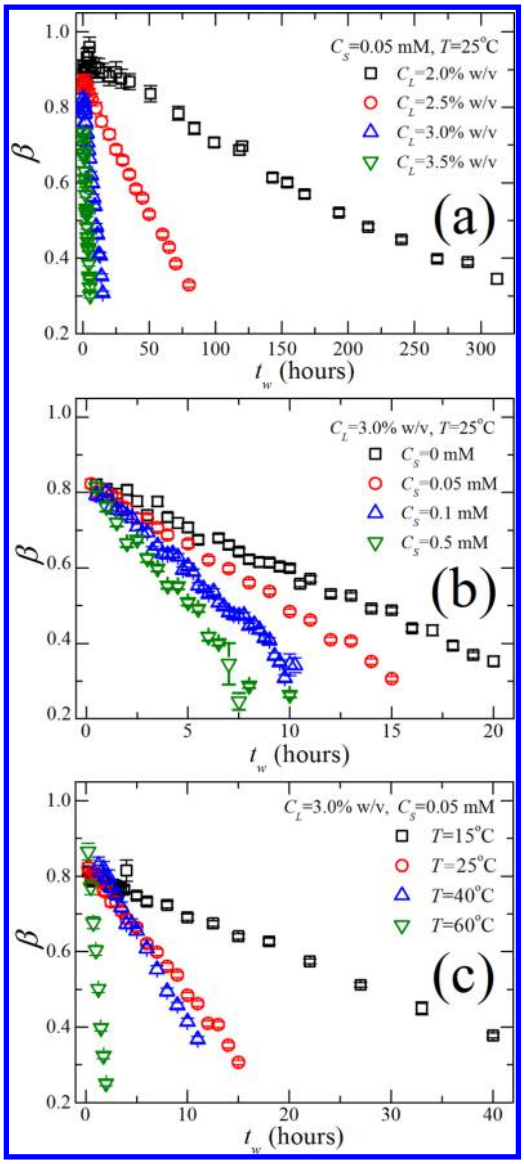

Figure 4. Stretching exponents β plotted vs t_w for different (a) C_L, (b) C_S, and (c) T values.

Figure 5a clearly shows that τ_1 has a nonmonotonic aging behavior with a minimum at small t_w. The initial decrease in τ_1 indicates that faster motion of the particle within its cage. Interestingly, $\langle\tau_{ww}\rangle$ remains almost constant over the same duration. We believe that the decrease in τ_1 originates from the delamination of Laponite particles at early times, a scenario that has been reported earlier.[20,46] It is seen from Figure 5 that τ_1 and $\langle\tau_{ww}\rangle$ increase simultaneously before they eventually diverge. This observation suggests that the enhancements in both of the relaxation time scales are correlated. For a material with purely repulsive interparticle interactions, the fast time scale is expected to remain finite, whereas the slow time scale diverges as the system approaches structural arrest. It is also seen in Figure 4 that β decreases linearly with t_w and the decay becomes faster with increase in C_L, C_S, and T. $\beta = 1$ represents a simple exponential decay with a single dominating relaxation time, whereas $\beta < 1$ indicates a broadening of the distribution of relaxation times with t_w.[45] Usually, glasses formed by dominating repulsive interactions are known to preserve the shapes of the relaxation time distributions during aging. This has been confirmed for polymer glasses,[47,48] spin glasses,[49] colloidal glasses with hard sphere interactions,[50] microgel pastes,[51] and concentrated emulsions.[52] On the other hand, chemical gels with covalent bonds between the polymeric chains and attractive colloidal gels are known to undergo broadening of their relaxation time distributions as a function of time.[53−56] Clearly, the spontaneously evolving young Laponite suspensions studied here show features that can be identified with colloidal gelation. Hence, the observations from our DLS experiments indicate an influence of attractive interactions. The correlation between τ_1 and $\langle\tau_{ww}\rangle$ and the decrease in β with t_w also remarkably corroborate the rheological observations reported earlier, where the influence of attraction is clearly visible for older rejuvenated Laponite suspensions and the process of structure formation is faster for higher values of C_L, C_S, and T.[30,57,58]

It is necessary to quantify the interaction potentials between Laponite particles to verify the influence of attractive interactions postulated from the DLS experiments. We next estimate the concentrations of Na^+ present in the aging Laponite suspensions of different C_L, C_S, and T. Na^+ in the

DOI: 10.1021/acs.langmuir.5b00291
Langmuir 2015, 31, 3012−3020

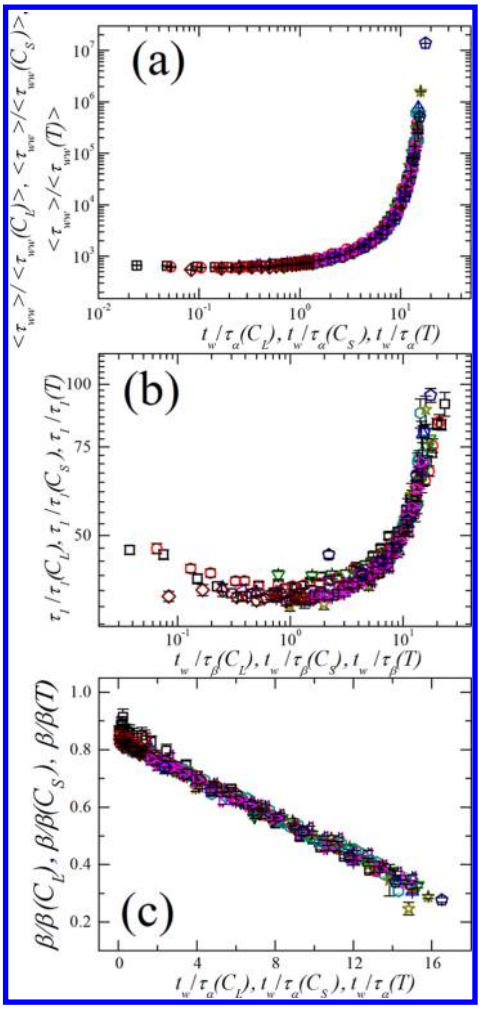

Figure 5. (a) Comprehensive superposition of scaled mean slow relaxation times $\langle\tau_{ww}\rangle/\langle\tau_{ww}(C_L)\rangle$, $\langle\tau_{ww}\rangle/\langle\tau_{ww}(C_S)\rangle$, and $\langle\tau_{ww}\rangle/\langle\tau_{ww}(T)\rangle$ plotted vs waiting time $t_w/\tau_\alpha(C_L)$, $t_w/\tau_\alpha(C_S)$, and $t_w/\tau_\alpha(T)$. Here, $\langle\tau_{ww}(C_L)\rangle$, $\langle\tau_{ww}(C_S)\rangle$, and $\langle\tau_{ww}(T)\rangle$ are, respectively, the vertical shift factors for $\langle\tau_{ww}\rangle$ when C_L, C_S, and T are changed, and $\tau_\alpha(C_L)$, $\tau_\alpha(C_S)$, and $\tau_\alpha(T)$ are the corresponding horizontal shift factors (plotted in Figure S1b,d,f). (b) Comprehensive superposition of scaled fast relaxation times $\tau_1/\tau_1(C_L)$, $\tau_1/\tau_1(C_S)$, and $\tau_1/\tau_1(T)$ plotted vs scaled waiting time $t_w/\tau_\beta(C_L)$, $t_w/\tau_\beta(C_S)$, and $t_w/\tau_\beta(T)$. Here, $\tau_1(C_L)$, $\tau_1(C_S)$, and $\tau_1(T)$ are, respectively, the vertical shift factors for scaling τ_1 when C_L, C_S, and T are changed, and $\tau_\beta(C_L)$, $\tau_\beta(C_S)$, and $\tau_\beta(T)$ are the corresponding horizontal shift factors (plotted in Figure S2b,d,f). (c) Comprehensive superposition of scaled stretching exponents $\beta/\beta(C_L)$, $\beta/\beta(C_S)$, and $\beta/\beta(T)$ plotted vs scaled waiting times $t_w/\tau_\alpha(C_L)$, $t_w/\tau_\alpha(C_S)$, and $t_w/\tau_\alpha(T)$. Here, $\beta(C_L)$, $\beta(C_S)$, and $\beta(T)$ are, respectively, the vertical shift factors for scaling β when C_L, C_S, and T are changed, and $\tau_\alpha(C_L)$, $\tau_\alpha(C_S)$, and $\tau_\alpha(T)$ are the corresponding horizontal shift factors (plotted in Figure S3b,d,f).

suspensions can originate from the externally added NaCl and from the dissociation of Na^+ from the faces of Laponite particles into the bulk aqueous medium. Since concentration of externally added NaCl (C_S) is known, an estimation of the time evolution of Na^+ ions can yield important information about the dissociation of Na^+ from the faces of the Laponite platelets. An estimation of the concentration of the dissociated Na^+ can be used to predict the amount of negative charges on the faces of the Laponite particles. The electronegativity of the Laponite particles, and hence the range of the electrostatic potential associated with the faces of these particles, can be then quantified by estimating the surface charge densities σ and the Debye screening lengths κ^{-1}. σ can be obtained by estimating the number of Na^+ dissociated per face of each Laponite particle and is given by $\sigma = e(n - n_0)/(2A_L n_p)$, where n_0 is the number density of ions due to the added salt, A_L is the area of the face of a Laponite particle (625 nm^2), and n_p is the number density of Laponite particles. κ^{-1} is given by $\kappa^{-1} = (\epsilon_0\epsilon_r k_B T/\sum_i (z_i e)^2 n_i)^{1/2}$,[2] where ϵ_0 is the permittivity of free space, ϵ_r is the relative permittivity of the medium, k_B is the Boltzmann constant, T is the temperature of the suspension, e is the charge of an electron, and z_i is the valence of the ith species of ions of concentration n_i. In aqueous suspensions of Laponite, two types of ions, Na^+ and Cl^-, influence κ^{-1}. The concentration of Na^+ in suspension is obtained using an ion meter, and the concentration of Cl^- ions is known a priori because C_S is fixed in every experiment.

The concentrations of Na^+, measured for Laponite suspensions at different C_L, C_S, and T, were used to extract σ and κ^{-1} values associated with the Laponite particles. Interestingly, for all Laponite suspensions, the concentrations of Na^+ progressively increases as a function of time (Figure 6a,d,g). This indicates a continuous dissociation of Na^+ from the faces of Laponite particles with increasing t_w. This results in a continuous temporal change in σ and κ^{-1} with changes in C_L, C_S, and T (Figure 6). For a given t_w, the Na^+ concentration is higher for greater C_L, C_S, and T (Figure 6a,d,g). Increasing C_L, C_S, and T, therefore, all result in increased dissociation of Na^+ and enhancement of the surface charge density of the Laponite particles (Figure 6b,e,h). The larger number of Na^+ in suspension enhances the screening and decreases the values of κ^{-1}, as observed in Figure 6c,f,i.

To understand the effects of the enhanced electronegativity of the faces of Laponite particles with increasing C_L, C_S, and T and the observed decrease in the Debye screening lengths, we solve the DLVO model for a scenario in which two plates approach each other in a parallel fashion. The total free energy per unit area, due to van der Waals attraction (W_{vdW}) and double-layer repulsion (W_{DL}) between the two layers of a 2:1 layer clay for weak interactions (i.e., κd large), is given by[3]

$$W(d) = W_{vdW} + W_{DL} = -\frac{A_H}{48\pi}\left[\frac{1}{d^2} + \frac{1}{(d+\Delta)^2} - \frac{2}{(d+\Delta/2)^2}\right] + \left(\frac{64 n k_B T}{\kappa}\right)\gamma^2 e^{-2\kappa d} \quad (2)$$

Here, A_H is the Hamaker constant (1.06×10^{-20} J), d is the half-distance between two Laponite platelets, as shown in Figure 7, Δ is the thickness of unit layers measured between the same planes (6.6 Å),[3] $\gamma = \tanh(ze\Phi_0/4k_BT)$, Φ_0 is the surface electric potential. Φ_0 is related to σ by $\sigma = e(n - n_0)/2A_L n_p = (8\epsilon_0\epsilon_r k_B T n)^{1/2} \sinh(ze\Phi_0/2k_BT)$.[3]

In Figure 7, we plot the total free energy of interaction $W(d)$ vs the half-distance d between the Laponite platelets for a 3.0% w/v Laponite suspension with 0.1 mM salt at 25 °C for different t_w. It can be seen that the height of the repulsive barrier increases with the passage of time. However, it can be simultaneously observed that the width of the repulsive barrier decreases with t_w. In the inset, we have shown the contribution from the different parts (repulsive (W_{DL}), attractive (W_{vdW}), and combined ($W_{DL} + W_{vdW}$)) to the total free energy. Clearly,

DOI: 10.1021/acs.langmuir.5b00291
Langmuir 2015, 31, 3012−3020

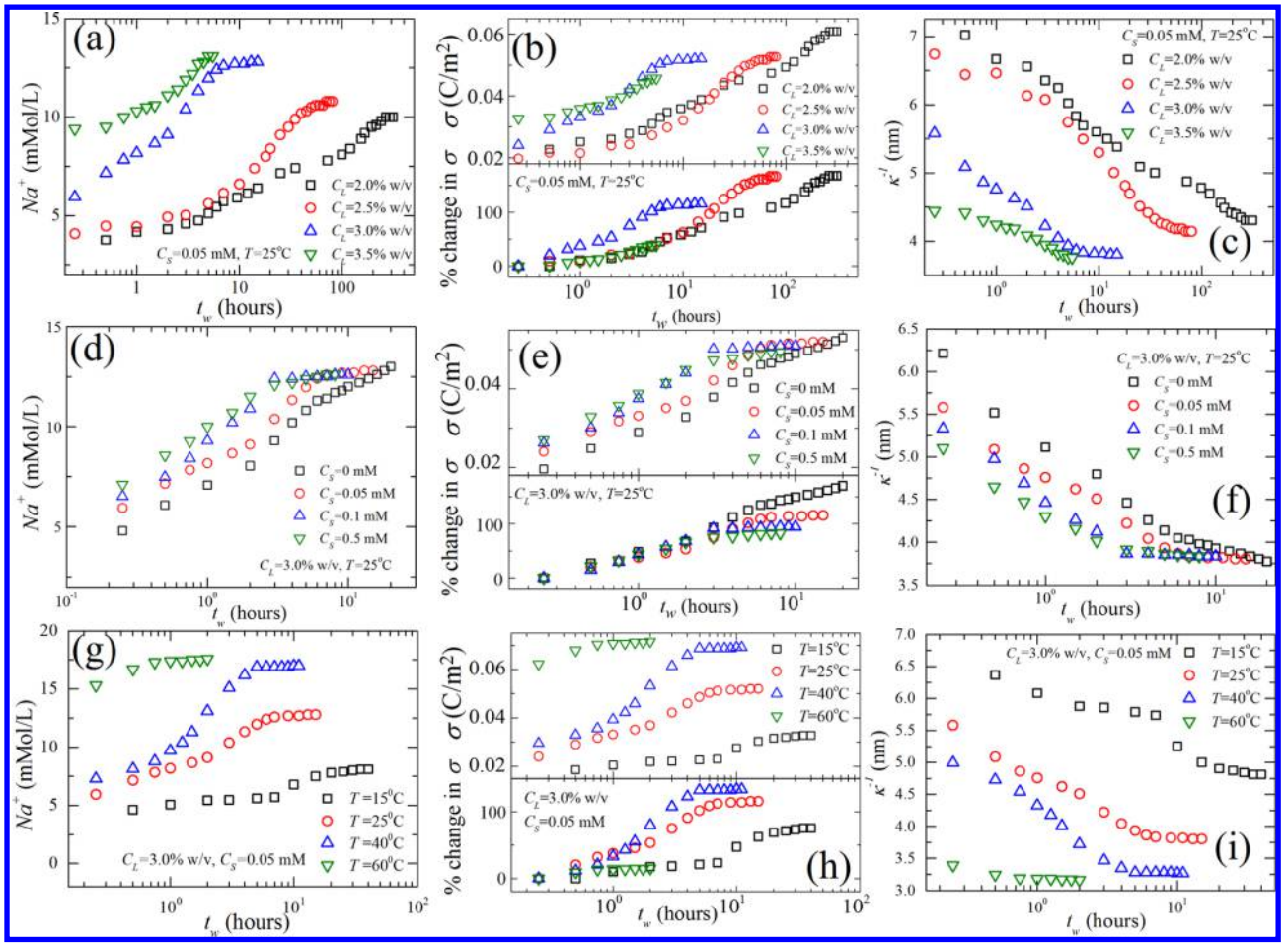

Figure 6. (a, d, g) Sodium ion concentration (Na^+), (b, e, h) surface charge density (σ), and (c, f, i) Debye screening length (κ^{-1}) plotted vs t_w for different (a–c) C_L, (d–f) C_S, and (g–i) T values.

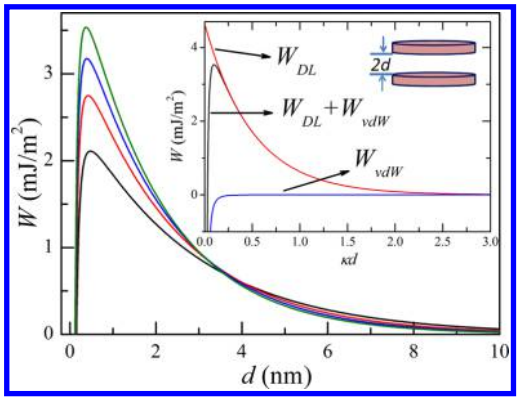

Figure 7. Free energy per unit area (W) between two layers of 2:1 Laponite clay (planar surfaces) calculated from DLVO theory and plotted as a function of half the distance, d, between Laponite platelets for a 3.0% w/v Laponite suspension with 0.1 mM salt at 25 °C at different waiting times t_w (from top to bottom: 10.0, 5.0, 1.5, and 0.25 h). In the inset, the free energy per unit area for the double-layer repulsive interaction W_{DL}, attractive van der Waals interaction W_{vdW}, and the combined interaction $W_{DL} + W_{vdW}$ are plotted vs κd for the same sample at t_w = 10.0 h.

the effect of the van der Waals interaction is negligible except in the limit of $d \ll \kappa^{-1}$.

For a Laponite suspension of fixed C_L and C_S, an increase in T leads to an increase in the concentration of dissociated Na^+ counterions. Therefore, the predictions of the DLVO theory for different temperatures will also be qualitatively similar to the results plotted in Figure 7, with t_w replaced by T.[20] Consequently, an increase in T is expected to cause an increase in the repulsive energy barrier while simultaneously decreasing the barrier width. Unlike temperature T and waiting time t_w, a change in the concentration of salt, C_S, keeps the value of γ unaffected. However, since $1/\kappa \approx 1/n^{1/2}$, the coefficient nk_BT/κ in eq 2 increases with increase in concentration of salt according to $nk_BT/\kappa \approx n^{1/2}$. Consequently, the qualitative behavior of the free energy per unit area calculated using DLVO theory with increase in C_S will be the same as that shown in Figure 7 but with t_w replaced by C_S. Similarly, an increase in C_L, the concentration of Laponite, causes an increase in n, and since $nk_BT/\kappa \approx n^{1/2}$, the qualitative behavior of the interparticle potential is again expected to remain the same as that shown in Figure 7 but with t_w replaced by C_L.

Microscopically, aqueous suspensions of Laponite consist of randomly-oriented disk-like particles that interact via face-to-face repulsive interactions, edge-to-face attractive interactions, and van der Waals interactions. The physical cages in which the individual particles are arrested can be represented as energy wells. The complex interparticle interaction between the anisotropic particles results in a distribution of well depths in the samples free-energy landscape. As the suspension is not in the lowest free energy state, Laponite particles continue to undergo microscopic motions as t_w increases. This gives rise to

DOI: 10.1021/acs.langmuir.5b00291
Langmuir 2015, 31, 3012–3020

structural rearrangements, or physical aging, and results in the eventual occupation of those states that have lower energy. If E is the mean energy well depth, then the cage diffusion or the slow time scale can simply be represented by $\langle\tau_{ww}\rangle = \langle\tau_{ww}\rangle_0 \exp(E/k_BT)$. Consequently, the increase in $\langle\tau_{ww}\rangle$, which represents an increase in the mean energy well depth, is a manifestation of a physical aging process. In this process, the time scale associated with the microscopic dynamics, which sets a unit time scale for the physical aging process, is represented by a microscopic time scale τ_m.[59] The time dependence of the mean energy well depth can then be represented by $E = E(t_w/\tau_m)$. The microscopic time scale τ_m, which is a measure of the rate of the evolution of $\langle\tau_{ww}\rangle$, can also be considered to have an Arrhenius temperature dependence given by $\tau_m = \tau_{m0} \exp(U/k_BT)$.[30] Here, U, the activation energy barrier associated with microscopic motion, sets the aging time scale τ_m and is distinct from E, the average depth of the energy well in which the particles reside.[30] As reported earlier, the self-similar evolution of $\langle\tau_{ww}\rangle$ shifts to lower waiting times with an increase in C_L, C_S, and T. Therefore, the shift factors associated with the time axis shown in Figures 2 and 5a can be related to the microscopic time scale as $\tau_m = \tau_m(C_L,C_S,T)$. Consequently, as per dependencies described in Figures S1b,d,f, it can be concluded that τ_m decreases with an increase in these variables. A decrease in τ_m indicates that the activation barrier U for microscopic motion decreases with an increase in C_L and C_S. As already noted, the aging behavior of Laponite suspensions is affected by T even more strongly. First, τ_m decreases with increase in T through the Arrhenius relationship cited earlier.[30] An increase in T also results in an increase in the concentration of Na^+ in suspension. Therefore, any change in T is expected to strongly affect the activation barrier U.

The results of our light scattering study and DLVO analysis, therefore, present a very interesting scenario. The light scattering study clearly suggests that the activation energy U, associated with microscopic motion of the particles, sets a time scale τ_m for structural reorganization events, which determines the rate of aging. This time scale (τ_m) decreases with increasing C_L, C_S, and T as mentioned before, accelerating the aging dynamics. A decrease in τ_m, in turn, indicates a decrease in U. Furthermore, due to its Arrhenius temperature dependence, τ_m is expected to decrease with increase in T. However, the DLVO analysis shows that C_L, C_S, and T not only cause an enhancement in the height of the repulsive potential but also lead to a shrinkage in the width of the repulsive potential. Therefore, the very fact that increasing C_L, C_S, and T results in a decrease in the width of the repulsive barrier, leading to accelerated structure formation (or a decrease in U), clearly indicates that the formed structure cannot be only repulsion-dominated. It is also important to note here that although the DLVO analysis presented here is for high Laponite concentrations (C_L > 2.0% w/v), qualitative features of DLVO analysis should be identical for low Laponite concentrations (C_L < 2.0% w/v) as well. It is, however, well-established that for low Laponite concentrations (C_L < 2.0% w/v) the microstructure of the suspension is attraction-dominated.[8] However, at low concentrations, the approach to an arrested state becomes considerably delayed due to the presence of a smaller number of Laponite particles.

We note that the predictions of DLVO theory are applicable strictly to the case when two Laponite particles approach each other in a parallel fashion, as shown in the inset of Figure 7. The DLVO interaction in the present case can be solved only for two parallel plates approaching each other. However, if the particles approach nonparallely, then the edge-to-face attraction will increase. Furthermore, since increase in C_L, C_S, T, and t_w lead to more electronegative faces, the nonparallel orientations will give rise to an enhanced decrease in the energy barrier U associated with structure formation. Hence, for all orientations of Laponite particles, attractive interaction will have an important influence on the low-energy structures.

CONCLUSIONS

In this work, we use dynamic light scattering to study the fast and slow relaxation time scale behavior of young Laponite suspensions as a function of the aging or waiting times t_w. The time evolution of the relaxation processes of young Laponite suspensions under various physicochemical conditions were investigated by changing the Laponite concentration C_L, the salt concentration C_S, and the suspension temperature T using both DLS and Na^+ measurements. Our data shows that both the fast and slow relaxation processes are self-similar upon changing C_L, C_S, and T. The stretching exponents β, associated with slow relaxation time scales, also show self-similarity. The Laponite concentration−salt concentration−temperature−time superpositions obtained here highlight the self-similar nature of the energy landscapes of Laponite suspensions when these physicochemical variables are changed. We also see signatures of a delamination effect of Laponite particles at early time when all of these variables are changed.

For aqueous suspensions of Laponite without externally added salt, small-angle X-ray scattering has established the presence of a repulsive glass at Laponite concentrations above 2 wt %,[28] where the particles do not touch each other and remain self-suspended. Also, dissolution[36] and rheological studies[30] showed that young Laponite suspensions (t_w < 2−3 days) are primarily repulsion-dominated, whereas attractive interactions strongly influence the structures of old samples (3 days < t_w < 7 days). The present study combines DLS, Na^+ measurements, and DLVO analysis to show that even for young suspensions (t_w < 2 days) the effect of attractive interactions is not negligible. However, it is extremely likely that the attractive interactions in young Laponite suspensions are weaker than the solvation forces that are likely to have dominated in the dissolution experiments mentioned above.[36] While this work gives unique insight into the possible structure of the arrested state, it still cannot give direct structural information. In any case, we believe that the present study complements several previous reports on the aging of aqueous suspensions of Laponite by suggesting that in an overall repulsive environment the attractive interactions between Laponite particles in aqueous suspension play an extremely influential role in exploring low-energy structures.

ASSOCIATED CONTENT

Supporting Information

Section A: Discussion of sodium ion measurement. Section B: Discussion of zeta potential measurement of the Laponite suspension. Section C: Discussion of the two-step relaxation process in glass formers and the mapping between waiting time t_w of Laponite suspension with inverse of temperature ($1/T$) of supercooled liquids. Figures S1−S3: Plots of the superpositions of $\langle\tau_{ww}\rangle$, τ_1, and β and the corresponding horizontal and vertical shift factors, respectively. Figure S4: Reproducibility of acquired autocorrelation functions. This material is available free of charge via the Internet at http://pubs.acs.org.

DOI: 10.1021/acs.langmuir.5b00291
Langmuir 2015, 31, 3012−3020

AUTHOR INFORMATION

Corresponding Authors

*(R.B.) E-mail: ranjini@rri.res.in,joshi@iitk.ac.in.
*(Y.M.J.) E-mail: joshi@iitk.ac.in.

Notes

The authors declare no competing financial interest.

ACKNOWLEDGMENTS

The authors thank R. Basak and S. Ali for their help with the experiments.

REFERENCES

(1) Evans, D. F.; Wennerstrom, H. *The Colloidal Domain*; Wiley VCH: New York, 1994.
(2) Israelachvili, J. N. *Intermolecular and Surface Forces*; Academic Press: New York, 2010.
(3) Olphen, H. V. *An Introduction to Clay Colloid Chemistry*; Wiley: New York, 1977.
(4) Hunter, G. L.; Weeks, E. R. The physics of the colloidal glass transition. *Rep. Prog. Phys.* **2012**, *75*, 066501.
(5) Kroon, M.; Wegdam, G. H.; Sprik, R. Dynamic light scattering studies on the sol-gel transition of a suspension of anisotropic colloidal particles. *Phys. Rev. E* **1996**, *54*, 6541−6550.
(6) Tawari, S. L.; Koch, D. L.; Cohen, C. Electrical double-layer effects on the Brownian diffusivity and aggregation rate of Laponite clay particles. *J. Colloid Interface Sci.* **2001**, *240*, 54−66.
(7) Jatav, S.; Joshi, Y. M. Chemical stability of Laponite in aqueous media. *Appl. Clay Sci.* **2014**, *97-98*, 72−77.
(8) Ruzicka, B.; Zaccarelli, E. A fresh look at Laponite phase diagram. *Soft Matter* **2011**, *7*, 1268−1286.
(9) Delhorme, M.; Jönsson, B.; Labbez, C. Monte Carlo simulations of a clay inspired model suspension: the role of rim charge. *Soft Matter* **2012**, *8*, 9691−9704.
(10) Delhorme, M.; Jönsson, B.; Labbez, C. Gel, glass and nematic states of plate-like particle suspensions: charge anisotropy and size effects. *RSC Adv.* **2014**, *4*, 34793−34800.
(11) Abou, B.; Bonn, D.; Meunier, J. Aging dynamics in a colloidal glass. *Phys. Rev. E* **2001**, *64*, 215101−215106.
(12) Bandyopadhyay, R.; Liang, D.; Yardimci, H.; Sessoms, D. A.; Borthwick, M. A.; Mochrie, S. G. J.; Harden, J. L.; Leheny, R. L. Evolution of particle-scale dynamics in an aging clay suspension. *Phys. Rev. Lett.* **2004**, *93*, 228302.
(13) Schosseler, F.; Kaloun, S.; Skouri, M.; Munch, J. P. Diagram of the aging dynamics in laponite suspensions at low ionic strength. *Phys. Rev. E* **2006**, *73*, 021401.
(14) Cocard, S.; Tassin, J. F.; Nicolai, T. Dynamical mechanical properties of gelling colloidal disks. *J. Rheol.* **2000**, *44*, 585−594.
(15) Joshi, Y. M.; Reddy, G. R. K.; Kulkarni, A. L.; Kumar, N.; Chhabra, R. P. Rheological behavior of aqueous suspensions of Laponite: new insights into the ageing phenomena. *Proc. R. Soc. A* **2008**, *464*, 469−489.
(16) Bandyopadhyay, R.; Mohan, P. H.; Joshi, Y. M. Stress relaxation in aging soft colloidal glasses. *Soft Matter* **2010**, *6*, 1462−1468.
(17) Bonn, D.; Tanase, S.; Abou, B.; Tanaka, H.; Meunier, J. Laponite: aging and shear rejuvenation of a colloidal glass. *Phys. Rev. Lett.* **2002**, *89*, 015701.
(18) McKenna, G. B.; Narita, T.; Lequeux, F. Soft colloidal matter: a phenomenological comparison of the aging and mechanical responses with those of molecular glasses. *J. Rheol.* **2009**, *53*, 489−516.
(19) Joshi, Y. M. Dynamics of colloidal glasses and gels. *Annu. Rev. Chem. Biomol. Eng.* **2014**, *5*, 181−202.
(20) Saha, D.; Joshi, Y. M.; Bandyopadhyay, R. Investigation of the dynamical slowing down process in soft glassy colloidal suspensions: comparisons with supercooled liquids. *Soft Matter* **2014**, *10*, 3292−3300.
(21) Bonn, D.; Kellay, H.; Tanaka, H.; Meunier, G. W.; Laponite, J. What is the difference between a gel and a glass. *Langmuir* **1999**, *15*, 7534−7536.
(22) Nicolai, T.; Cocard, S. Light scattering study of the dispersion of Laponite. *Langmuir* **2000**, *16*, 8189−8193.
(23) Ruzicka, B.; Zulian, L.; Ruocco, G. More on the phase diagram of Laponite. *Langmuir* **2006**, *22*, 1106−1111.
(24) Cummins, H. Z. Liquid, glass, gel: the phases of colloidal Laponite. *J. Non-Cryst. Solids* **2007**, *353*, 3891−3905.
(25) Jabbari-Farouji, S.; Tanaka, H.; Wegdam, G. H.; Bonn, D. Multiple nonergodic disordered states in Laponite suspensions: a phase diagram. *Phys. Rev. E* **2008**, *78*, 061405−061410.
(26) Angelini, R.; Zulian, L.; Fluerasu, A.; Madsen, A.; Ruocco, G.; Ruzicka, B. Dichotomic aging behaviour in a colloidal glass. *Soft Matter* **2013**, *9*, 10955−10959.
(27) Strachan, D. R.; Kalur, G. C.; Raghavan, S. R. Size-dependent diffusion in an aging colloidal glass. *Phys. Rev. E* **2006**, *73*, 041509.
(28) Ruzicka, B.; Zulian, L.; Angelini, R.; Sztucki, M.; Moussaid, A.; Ruocco, G. Arrested state of clay-water suspensions: gel or glass? *Phys. Rev. E* **2008**, *77*, 020402−020404.
(29) Mourchid, A.; Delville, A.; Lambard, J.; Lecolier, E.; Levitz, P. Phase diagram of colloidal dispersions of anisotropic charged particles: equilibrium properties, structure, and rheology of laponite suspensions. *Langmuir* **1995**, *11*, 1942−1950.
(30) Shahin, A.; Joshi, Y. M. Physicochemical effects in aging aqueous laponite suspensions. *Langmuir* **2012**, *28*, 15674−15686.
(31) Shahin, A.; Joshi, Y. M. Irreversible aging dynamics and generic phase behavior of aqueous suspensions of Laponite. *Langmuir* **2010**, *26*, 4219−4225.
(32) Rich, J. P.; McKinley, G. H.; Doyle, P. S. Size dependence of microprobe dynamics during gelation of a discotic colloidal clay. *J. Rheol.* **2011**, *55*, 273−299.
(33) Negi, A. S.; Osuji, C. Time-resolved viscoelastic properties during structural arrest and aging of a colloidal glass. *Phys. Rev. E* **2010**, *82*, 031404.
(34) Negi, A. S.; Osuji, C. Dynamics of a colloidal glass during stress-mediated structural arrest. *Europhys. Lett.* **2010**, *90*, 28003.
(35) Mongondry, P.; Tassin, J. F.; Nicolai, T. Revised state diagram of Laponite dispersions. *J. Colloid Interface Sci.* **2005**, *283*, 397−405.
(36) Ruzicka, B.; Zulian, L.; Zaccarelli, E.; Angelini, R.; Sztucki, M.; Moussaïd, A.; Ruocco, G. Competing interactions in arrested states of colloidal clays. *Phys. Rev. Lett.* **2010**, *104*, 085701.
(37) Berne, B. J.; Pecora, R. *Dynamic Light Scattering: With Applications to Chemistry, Biology, and Physics*; John Wiley & Sons: New York, 1975.
(38) Angell, C. A.; Ngai, K. L.; McKenna, G. B.; McMillan, P. F.; Martin, S. W. Relaxation in glassforming liquids and amorphous solids. *J. Appl. Phys.* **2000**, *88*, 3113−3157.
(39) Ngai, K. L. Relation between some secondary relaxations and the α relaxations in glass-forming materials according to the coupling model. *J. Chem. Phys.* **1998**, *109*, 6982.
(40) Debenedetti, P.; Stillinger, F. H. Supercooled liquids and the glass transition. *Nature* **2001**, *410*, 259−267.
(41) Kudlik, A.; Tschirwitz, C.; Benkhof, S.; Blochowicz, T.; Rössler, E. Slow secondary relaxation process in supercooled liquids. *Europhys. Lett.* **1997**, *40*, 649−654.
(42) Ruzicka, B.; Zulian, L.; Ruocco, G. Ergodic to non-ergodic transition in low concentration Laponite. *J. Phys.: Condens. Matter* **2004**, *16*, S4993−S5002.
(43) Ruzicka, B.; Zulian, L.; Ruocco, G. Routes to gelation in a clay suspension. *Phys. Rev. Lett.* **2004**, *93*, 258301.
(44) Gotze, W.; Sjogren, L. Relaxation processes in supercooled liquids. *Rep. Prog. Phys.* **1992**, *55*, 241−376.
(45) Lindsey, C. P.; Patterson, G. Detailed comparison of the Williams−Watts and Cole−Davidson functions. *J. Chem. Phys.* **1980**, *73*, 3348−3357.
(46) Ali, S.; Bandyopadhyay, R. Use of ultrasound attenuation spectroscopy to determine the size distribution of clay tactoids in aqueous suspensions. *Langmuir* **2013**, *29*, 12663−12669.

DOI: 10.1021/acs.langmuir.5b00291
Langmuir 2015, 31, 3012−3020

(47) Struik, L. C. E. *Physical Aging in Amorphous Polymers and Other Materials*; Elsevier: Amsterdam, 1978.
(48) Joshi, Y. M. Long time response of aging glassy polymers. *Rheol. Acta* **2014**, *53*, 477−488.
(49) Rodriguez, G. F.; Kenning, G. G.; Orbach, R. Full aging in spin glasses. *Phys. Rev. Lett.* **2003**, *91*, 037203.
(50) Derec, C.; Ducouret, G.; Ajdari, A.; Lequeux, F. Aging and nonlinear rheology in suspensions of polyethylene oxide-protected silica particles. *Phys. Rev. E* **2003**, *67*, 061403.
(51) Cloitre, M.; Borrega, R.; Leibler, L. Rheological aging and rejuvenation in microgel pastes. *Phys. Rev. Lett.* **2000**, *85*, 4819.
(52) Shahin, A.; Joshi, Y. M. Prediction of long and short time rheological behavior in soft glassy materials. *Phys. Rev. Lett.* **2011**, *106*, 038302.
(53) Winter, H. H. Glass transition as the rheological inverse of gelation. *Macromolecules* **2013**, *46*, 24252432.
(54) Hodgson, D. F.; Amis, E. J. Dynamic viscoelasticity during sol-gel reactions. *J. Non-Cryst. Solids* **1991**, *131*, 913−920.
(55) Choi, J. H.; Ko, S.-W.; Kim, B. C.; Blackwell, J.; Lyoo, W. S. Phase behavior and physical gelation of high molecular weight syndiotactic poly(vinyl alcohol) solution. *Macromolecules* **2001**, *34*, 2964−2972.
(56) Ponton, A.; Bee, A.; Talbot, D.; Perzynski, R. Regeneration of thixotropic magnetic gels studied by mechanical spectroscopy: the effect of the pH. *J. Phys.: Condens. Matter* **2005**, *17*, 821−836.
(57) Jatav, S.; Joshi, Y. M. Rheological signatures of gelation and effect of shear melting on aging colloidal suspension. *J. Rheol.* **2014**, *58*, 1535.
(58) Shahin, A.; Joshi, Y. M. Hyper-aging dynamics of nanoclay suspension. *Langmuir* **2012**, *28*, 5826.
(59) Fielding, S. M.; Sollich, P.; Cates, M. E. Aging and rheology in soft materials. *J. Rheol.* **2000**, *44*, 323−369.

DOI: 10.1021/acs.langmuir.5b00291
Langmuir 2015, 31, 3012−3020